Journal of Power Sources 254 (2014) 323–328

Contents lists available at ScienceDirect

Journal of Power Sources

journal homepage: www.elsevier.com/locate/jpowsour

Chemical synthesis of PbO_2 particles with multiple morphologies and phases and their electrochemical performance as the positive active material

Na Fan [a], Changhui Sun [a,*], Delong Kong [c], Yitai Qian [a,b]

[a] Hefei National Laboratory for Physical Science at Microscale and Department of Chemistry, University of Science and Technology of China, Hefei 230026, China
[b] School of Chemistry and Chemical Engineering, Shandong University, Jinan 250100, China
[c] Shandong Sacred Sun Power Sources Industry Co. Ltd., Qufu 273100, China

HIGHLIGHTS

- PbO_2 particles with multiple morphologies and phases were chemically synthesized.
- The electrode made with β-PbO_2 and α-PbO_2 (1:1) displays better electrochemical performance.
- The electrode can deliver a capacity of 183 mA h g^{-1} at 0.1 C after 100 cycles.
- The pretreated electrode displays improved stability of cycle.

ARTICLE INFO

Article history:
Received 14 October 2013
Received in revised form
5 December 2013
Accepted 17 December 2013
Available online 25 December 2013

Keywords:
Lead dioxide
Positive material
Chemical synthesis
Lead acid battery

ABSTRACT

In order to explore how to improve the electrochemical performance of the lead-acid battery positive active material, PbO_2 particles with multiple morphologies and phases including urchin-like and ball-like β-PbO_2 particles with size of 0.5–1 μm, flower-like α-PbO_2 particles with size of 1–2 μm are chemically synthesized. These samples are composed of different smaller nanoparticles. The electrode made with urchin-like β-PbO_2 and flower-like α-PbO_2 in the ratio of 1:1 can deliver a discharge capacity of 183 mA h g^{-1} at 0.1 C after 100 cycles, and subsequent rate performance test shows that a discharge capacity of 97.2 mA h g^{-1} can be obtained even at 1 C. Moreover, this kind of electrode pretreated in 1 M H_2SO_4 solution displays improved stability of cycle, a capacity of 146.7 mA h g^{-1} can be obtained after 100 cycles, and its corresponding active material utilization ratio can reach 65%.

1. Introduction

The lead-acid battery has relatively lower energy and power densities, and poor cycling performance compared with other secondary batteries such as the Ni–MH or the Li-ion [1, 2]. However, we have to admit that the lead-acid battery is still the most widely used rechargeable batteries in the world due to its mature manufacturing technology, reliability and high safety. And most importantly, the energy cost of lead-acid battery is 2–3 times lower than that of other types of batteries [3]. Therefore, taking into account economic issues, it is easy to understand why the lead-acid battery occupies a dominant position on the market. Today, the development of solar, wind and other clean energy sources, as well as the micro hybrid electric vehicles brings more challenges for the lead-acid battery technology innovation [4–7]. Currently, lead–carbon battery technology is considered to be a promising solution, but it mainly focuses on the negative plates. As we all know, the traditional manufacturing process of lead-acid battery positive plate usually makes the utilization ratio of PbO_2 very low, and energy density in the range of only 30–40 W h kg^{-1} can be obtained [8–12]. To some extent these disadvantageous factors limit the application of lead-acid battery. Thereby, to improve the positive active materials and technology is imperative for advanced lead-acid batteries with higher discharge capacity and better cycling performance.

It is well established that the active mass on the positive plate after formation is composed of α-PbO_2 and β-PbO_2 [9, 10]. The α-PbO_2 crystals form the active mass skeleton, which play the role of

* Corresponding author. Tel./fax: +86 551 63607402.
E-mail address: chhsun@ustc.edu.cn (C. Sun).

0378-7753/$ – see front matter © 2013 Elsevier B.V. All rights reserved.
http://dx.doi.org/10.1016/j.jpowsour.2013.12.077

conducting the current throughout the positive active mass in the charge/discharge processes and ensure the cycle life of the lead-acid battery. The β-PbO_2 crystals are electrochemically active which determine the capacity of the positive plates. Consequently, the cooperation of the two types of PbO_2 is very important for the capacity and cycle life of the lead-acid battery [11,13]. Furthermore, recent studies have shown that the particle properties such as size, morphology and specific surface area of the electrode materials play an important role in the improvement of electrochemical activity of electrodes in batteries [14–16]. And it is generally accepted that the utilization ratio of the active mass can be increased by reducing the β-PbO_2 particle size to nano-scale and enhancing its surface area [17, 18]. The electrochemical activity of PbO_2 synthesized by chemical synthesis is relatively lower than that of PbO_2 obtained by electrochemical reaction [17,19,20]. But it is much easier to control the PbO_2 particle size, morphology, structure and adjust the ratio of α and β by chemical synthesis. Moreover, recent works have shown that the chemically prepared PbO_2 particles also can exhibit better electrochemical activity, only if the connections among the particles and between the particles and the current collector are built up using a proper method [15,16,21]. For example, Morales et al. [15] prepared the nanostructured electrode by spraying an aqueous suspension of 15–20 nm β-PbO_2 particles over the lead alloy sheets, the β-PbO_2 nanoparticles were obtained by hydrolysis of a $Pb(CH_3{-}COO)_4$ precursor, and the electrode exhibited high utilization of the active material (about 65% of the theoretical capacity on discharge with 1 C discharge current). Bervas et al. [16] constructed the mini-tubular electrodes using the nano β-PbO_2 with a high surface area of 26.4 $m^2\ g^{-1}$, the PbO_2 was synthesized by the chemical oxidation of lead(II) nitrate with ammonium persulfate in strong alkaline conditions. This tubular electrode displayed more than 45% utilization ratio of the positive active material and achieved excellent cycling stability in diluted H_2SO_4. de Andrade et al. [21] assembled a tubular electrode for lead acid batteries directly using nanometric PbO_2 particle which was also synthesized by hydrolysis of $Pb(CH_3{-}COO)_4$, and the electrode can maintain a high capacity of 180 A h kg^{-1} after more than 130 cycles. The former studies mainly focused on the nano β-PbO_2, however, the α-PbO_2 which plays the supporting and conducting role was rarely considered. Cui et al. [22] reported that the composite electrode made with α-PbO_2 and β-PbO_2 was beneficial to improve the charge/discharge performance, yet the electrochemical measurements were carried out using a three-electrode system. Furthermore, the utilization ratio of the active mass, capacity and cycle performance are not amply investigated.

In this work, urchin-like and ball-like β-PbO_2 particles with size of 0.5–1 μm, flower-like α-PbO_2 particle with size of 1–2 μm were chemically synthesized. The individual and synergistic effects of α-PbO_2 and β-PbO_2 on the discharge capacity were investigated. And the inherent relationship between morphology and electrochemical property of the electrode materials was explored. The electrodes pretreated by dilute sulfuric acid would provide improved cycling stability. At the same time, the electrodes showed very high utilization ratio of active material.

2. Experimental

2.1. Material preparation

2.1.1. Synthesis of urchin-like β-PbO_2

In a typical synthesis, 0.6 g $Pb(NO_3)_2$ and 0.5 g PVP were dissolved in 35 mL of deionized water, then 3.55 mL of 0.5 g mL^{-1} NaOH aqueous solution was added into the solution. The mixture was stirred strongly to form a transparent solution. Thereafter, 2 mL NaClO solution (available chlorine ≥5%) was added under constant stirring to form a homogeneous solution. The above solution was transferred into a 60 mL Teflon-lined autoclave, and the autoclave was sealed and maintained at 90 °C for 10 h. After the autoclave was cooled down to room temperature naturally, the resulting brown products were centrifuged and washed with deionized water and ethanol several times, subsequently dried at 60 °C for 4 h in air.

2.1.2. Synthesis of ball-like β-PbO_2

Typically, 1.48 mL of 0.1 g mL^{-1} NaOH aqueous solution was added into a round-bottom flask containing 80 mL of 0.033 mol L^{-1} $Pb(CH_3COO)_2{\cdot}3H_2O$ whilst stirring it mechanically, then a milk white suspension formed. After 5 min, 10 mL NaClO solution (available chlorine ≥5%) was poured into the flask, generating an orange colored suspension. Afterward, the flask was transferred into a magnetic stirring thermostat water bath, and maintained at 90 °C for 5 h. After cooling down to room temperature, the brown product was collected by centrifugation and washed with deionized water and ethanol, finally dried at 60 °C for 4 h in air.

2.1.3. Synthesis of flower-like α-PbO_2

Flower-like α-PbO_2 was prepared by a similar method reported elsewhere [22]. In our experiment, $(NH_4)_2S_2O_8$ was used as oxidant.

2.2. Characterization

The X-ray powder diffraction (XRD) patterns of the samples were characterized on a Bruker D8 advanced X-ray diffractometer equipped with graphite monochromatized Cu Kα radiation (Kα = 1.5418 Å). The scanning electron microscopy (SEM) images were taken by a JEOL JSM-7600F field emission instrument. The transmission electron microscopy (TEM) images were recorded on a JEM-1011 transmission electron microscope at an acceleration voltage of 100 kV.

2.3. Electrochemical performance test

The electrode for electrochemical studies was a thin film electrode which was prepared by pressing the mixture of 95 wt% of the synthesized PbO_2 and 5 wt% of poly(tetrafluoroethylene) (60 wt% solution) on to a Pb sheet, and then dried at 80 °C for 24 h. The amount of PbO_2 in each electrode was ca. 30 mg. The electrode was cycled in a laboratory mini-cell and the counter electrodes were two small conventional negative electrodes cut from a commercial plate. Compared to the positive electrode active mass, the negative electrode active mass was in large excess. The electrolyte was a H_2SO_4 solution with a relative density of 1.245 g mL^{-1}. The cycling tests were carried out on Land CT2001A according to the following procedure: discharge with 0.1 C until the voltage fell to 1.8 V; charge with 0.1 C until the voltage increased to 2.4 V; when the charger voltage was held constant at 2.4 V for 1 h another cycle began. The utilization ratio of the PbO_2 was evaluated with respect to a 100% theoretical capacity of 224 mA h g^{-1}.

3. Results and discussion

The XRD patterns of the as-prepared β-PbO_2 and α-PbO_2 products are shown in Fig. 1. All the diffraction peaks in Fig. 1a can be indexed to a pure tetragonal phase of β-PbO_2 (JCPDS card, No. 65-2826); while in the XRD pattern (Fig. 1b) except for the diffraction peaks of β-PbO_2, a peak at 28.5° can be seen obviously which should be ascribed to the existence of a small quantity of α-PbO_2. In Fig. 1c, it is observed that all the main diffraction peaks can be assigned to the orthorhombic phase of α-PbO_2 (JCPDS card, No. 45-1416). The strong and sharp reflection peaks in the three XRD

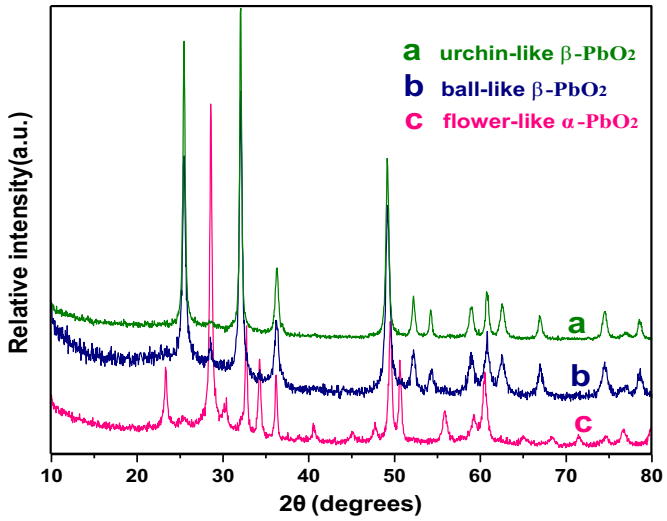

Fig. 1. XRD patterns of the samples.

patterns suggest that the obtained PbO_2 samples are well crystallized.

The morphology and microstructure of the as-prepared samples were further characterized by SEM. Fig. 2a shows a typical SEM image of uniform three-dimensional (3D) urchin-like micro spherical arrays with a diameter of 0.5–1 μm, which are self-assembled in a radial way by lots of aligned β-PbO_2 nanorods. The magnified SEM image (Fig. 2b) demonstrates that the average diameter and length of the nanorod building blocks can be identified as ca. 20 nm and 100 nm, respectively. At the same time the hollow structures can be seen very clearly from the broken particles in Fig. 2a and b. This is further supported by TEM (Fig. 2b, inset); careful contrast between the dark edge and pale center confirms the hollow structures of β-PbO_2 microspheres. Fig. 2c displays that the ball-like β-PbO_2 particles with rough surface are almost the same and their diameters are also ca. 0.5–1 μm. In Fig. 2d, it can be distinctly observed that these particles are constructed from many smaller nanoparticles with diameters of about 50–100 nm. Fig. 2e and f reveals that the as-prepared α-PbO_2 particles were composed of a large quantity of flower architectures with a size of 1–2 μm. Each flower is formed by many nano-scale pyramidal petals. The sizes of the big and small petals are ca. 500 nm and 100–200 nm, respectively. The clear-cut edge and non-smooth surface of the petals can be evidently observed in Fig. 2f.

The as-prepared electrodes were assembled into laboratory mini-cells to evaluate their electrochemical performances. As illustrated in Fig. 3, if the electrode made with β-PbO_2:α-PbO_2 (1:1) was charged/discharged at 0.1 C without the constant voltage charge step, only a capacity of 56.2 mA h g^{-1} can be obtained after 50 cycles, and the corresponding active material utilization ratio is 25%. However, when the charge condition was made a small change, i.e. holding constant at 2.4 V for 1 h, a visible experimental

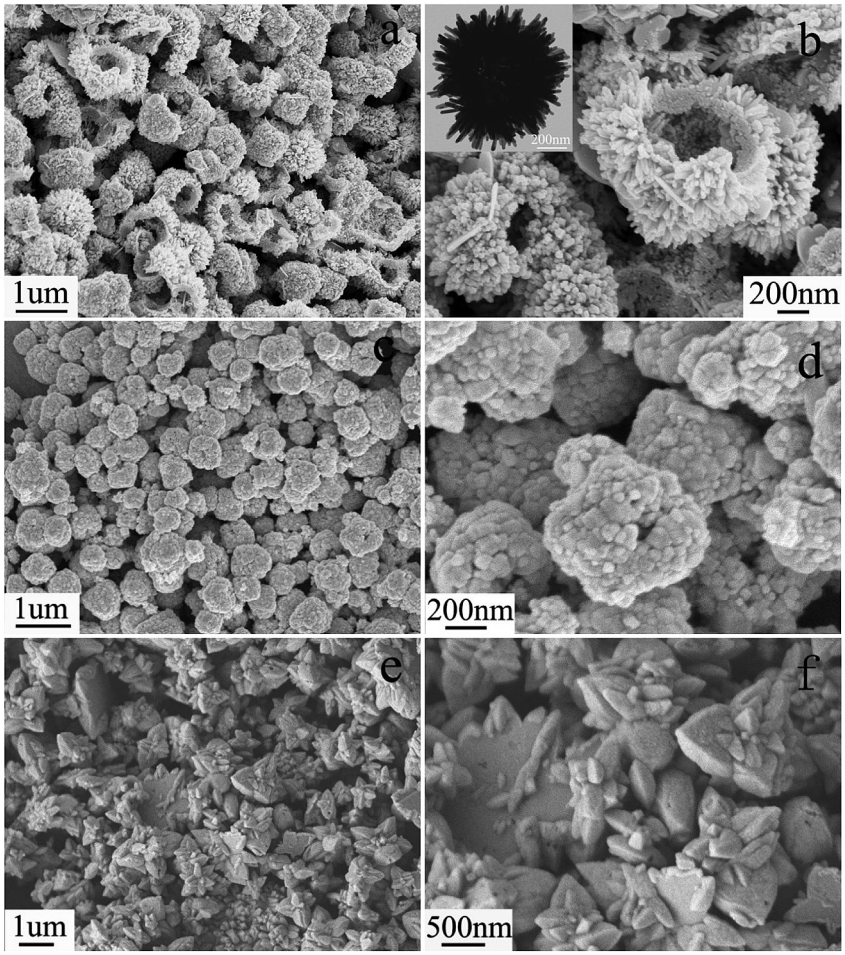

Fig. 2. SEM images of the samples: (a-b) urchin-like β-PbO_2, (c-d) ball-like β-PbO_2, (e-f) flower-like α-PbO_2.

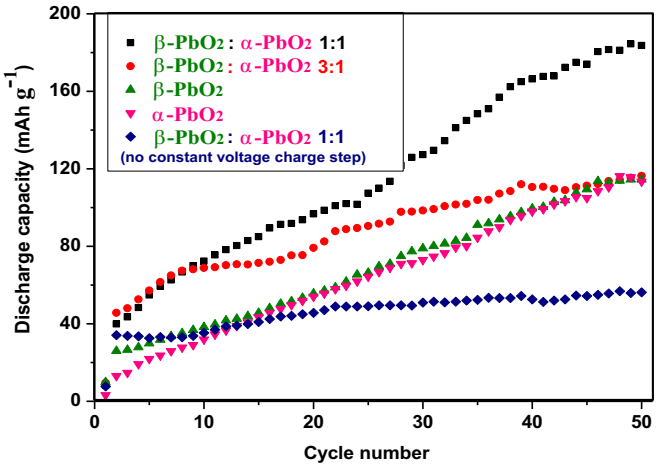

Fig. 3. Comparisons of discharge performance at different ratios and charge conditions. Urchin-like β-PbO_2 and flower-like α-PbO_2 are used to make contrasts.

phenomenon appears: the discharge capacity is markedly increased from the 2nd to 50th cycles. It reaches a very high capacity of 183.7 mA h g^{-1} at the 50th cycle. The above test results suggest that the constant voltage charge step can accelerate the conversion of partial α-PbO_2 to β-PbO_2 and build up the connection between particles, which will be beneficial to improve the discharge performance of the electrode. To further confirm whether the conversion of α-PbO_2 to β-PbO_2 has happened, the phases of the electrode material were characterized by XRD when the electrode executed certain cycles. As shown in Fig. 4b, the electrode made with urchin-like β-PbO_2 and flower-like α-PbO_2 in the ratio of 1:1 without constant voltage step after 50 cycles is composed of three phases: β-PbO_2, α-PbO_2 and $PbSO_4$, and by comparing the peak intensities of α-PbO_2 with that in Fig. 1c, we can concluded that most of α-PbO_2 reacted with the electrolyte producing $PbSO_4$. However, in Fig. 4a, the diffraction peaks of β-PbO_2 can be clearly observed, which means that the conversion of α-PbO_2 to β-PbO_2 really happened in the electrode made with only flower-like α-PbO_2 by the constant voltage charge step after 50 cycles. And the conversion is further confirmed by Fig. 4c, the electrode made with urchin-like β-PbO_2 and flower-like α-PbO_2 in the ratio of 1:1 after 100 cycles mainly consists of β-PbO_2, only one α-PbO_2 peak can be detected and it is very weak. In addition, Figs. 3 and 5 show that the electrodes prepared with these chemically synthesized lead dioxides have discharge capacities about or less than 40 mA h g^{-1} during the initial cycles. On further cycling, however, a significant increase in electrode discharge capacity to 150–180 mA h g^{-1} is observed after 50–100 cycles (Fig. 5). Moreover, the β-PbO_2 electrode itself exhibits a several-fold increase in discharge capacity, which indicates that its composition and structure are changed. According to the gel-crystal mechanism proposed by Pavlov [23–25], chemically synthesized PbO_2 has crystal structure, while the electrochemically produced PbO_2 particles contain crystal and hydrated (gel) zones, and this gel-crystal system possesses high electron and proton conductivities. The electrochemical reactions proceed in the gel zones of the PbO_2 active mass and thus greater volume of the lead dioxide is involved in the electrochemical processes and hence the electrode capacity is increased. Therefore, on the basis of our obtained experimental data, it can be concluded that the β-PbO_2 particles get hydrated and acquire the properties of electrochemically produced PbO_2. The formation of hydrated zones in the PbO_2 particles during cycling and their involvement in the electrochemical processes of charge and discharge should bear the primary responsibility for the higher electrode discharge capacity on cycling. The electrodes made with individual β-PbO_2 or α-PbO_2 have the similar discharge capacity curves except for the initial 10 cycles. Especially, the first discharge capacity of β-PbO_2 is 9.9 mA h g^{-1}, which is 3 times higher than that of α-PbO_2 (3.2 mA h g^{-1}). But with the progress of the cycle, the difference of discharge capacity value becomes smaller, which can be attributed to the conversion of α-PbO_2 to β-PbO_2. In comparison with individual β-PbO_2 electrodes the mixture electrodes made with β-PbO_2:α-PbO_2 (1:1 and 3:1) possess the remarkably higher capacity. The reason is that the presence of an appropriate amount of flower-like α-PbO_2 with larger particle size in positive active materials will help to construct the frame structure and form a conductive network in the electrode. Thereby, the discharge capacities of the initial cycles and the active material utilization ratio can be further enhanced. The electrode made with β-PbO_2:α-PbO_2 (1:1) contains more α-PbO_2 than that with β-PbO_2:α-PbO_2 (3:1), therefore, more frame structure and conductive network can be formed, which will make more β-PbO_2 get involved in the charge/

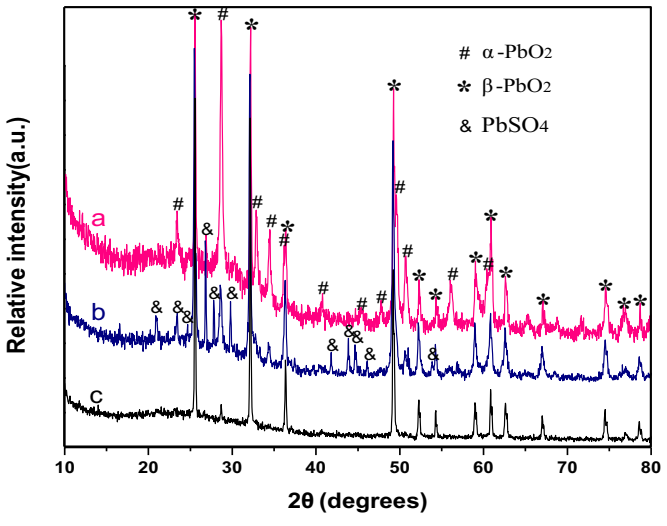

Fig. 4. XRD patterns of the electrodes: (a) flower-like α-PbO_2 after 50 cycles, (b) urchin-like β-PbO_2 and flower-like α-PbO_2 in the ratio of 1:1 with no constant voltage step after 50 cycles, (c) urchin-like β-PbO_2 and flower-like α-PbO_2 in the ratio of 1:1 after 100 cycles.

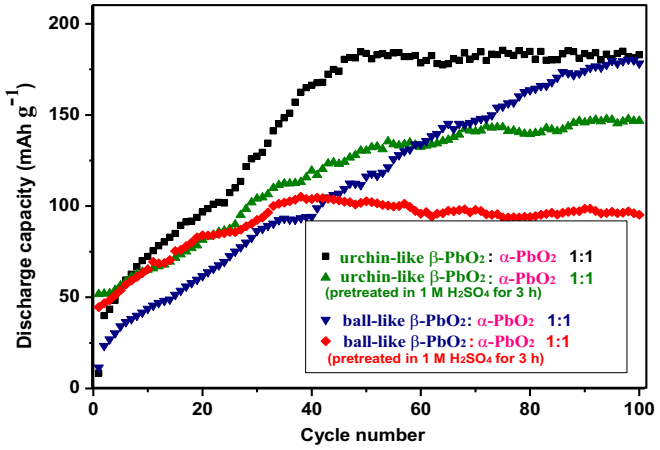

Fig. 5. Comparative cycle performances of urchin-like β-PbO_2, ball-like β-PbO_2 and flower-like α-PbO_2 in the ratio of 1:1. And the cycle behavior of the electrodes pretreated in 1 M H_2SO_4 solution for 3 h.

discharge reaction and as a result a relatively higher capacity is obtained. Anyway, the coexistence and proportion of α-PbO_2 and β-PbO_2 is indispensable to improve the electrochemical performance of positive electrode [26].

On the basis of the above experimental data analysis, the ratio of β-PbO_2:α-PbO_2 1:1 was adopted for further experimental studies. In order to investigate the effect of the morphologies of β-PbO_2 on the electrochemical property of the electrode, two kinds of electrodes were made using the as-prepared urchin-like and ball-like β-PbO_2 samples with the same proportion of α-PbO_2. As shown in Fig. 5, the two electrodes can deliver the discharge capacity of 183 mA h g^{-1} and 178.2 mA h g^{-1} after 100 cycles, respectively, which is close to the best result reported by Andrade et al. [21] and superior to the results in other literatures [16,27]. However, the cycle curve of the electrode made with urchin-like β-PbO_2 is much higher than that prepared with ball-like β-PbO_2. The special morphology and microstructure of the urchin-like β-PbO_2 sample should be responsible for the increased discharge capacity of the electrode. The two types of β-PbO_2 samples have almost the same particle size, but the particular hollow and radial nanorods structures of the urchin-like β-PbO_2 enlarge its surface area, which will lead to a large contact area between the active material and the electrolyte. Furthermore, the typical urchin-like structure can offer unique advantages for electrolyte storage and make fast diffusion of H^+ and SO_4^{2-} ions in the electrode. According to the literature report [21], the electrodes were pretreated by following the procedure: incubated in 1 M H_2SO_4 solution for 3 h, washed with deionized water, dried at 60 °C overnight, placed into the mini-cell, submitted to a charge current of 5.0 mA g^{-1} for 30 min and discharged to 1.8 V, and then the charge/discharge cycles began. It can be seen from Fig. 5 that the initial several discharge capacities of the two electrodes are visibly enhanced. And the two electrodes have the similar level in terms of discharge capacities during the initial 25 cycles. But compared with the electrode fabricated with ball-like β-PbO_2, the electrode made with urchin-like β-PbO_2 exhibits higher discharge capacity in the following cycles. Finally a capacity of 146.7 mA h g^{-1} can be obtained after 100 cycles, and its corresponding active material utilization ratio can reach 65%. Although the two electrodes after pretreatment display relatively lower discharge capacities, the difference in discharge capacity value is reduced from the 1st to the 100th cycles compared to the electrodes before pretreatment, so the stability of the holistic cycle curve is improved, which is very important for the practical application of electrode. There are some differences between our experimental results and the literature reports [21], this may be because the type of electrode used in our experiment is the thin film electrode, however, in the literature the tubular electrode is employed. Therefore, the similar pretreatment could cause difference impact on the electrode. Nevertheless, in general the pretreatment will help to establish connections among the particles and improve the stability of cycle.

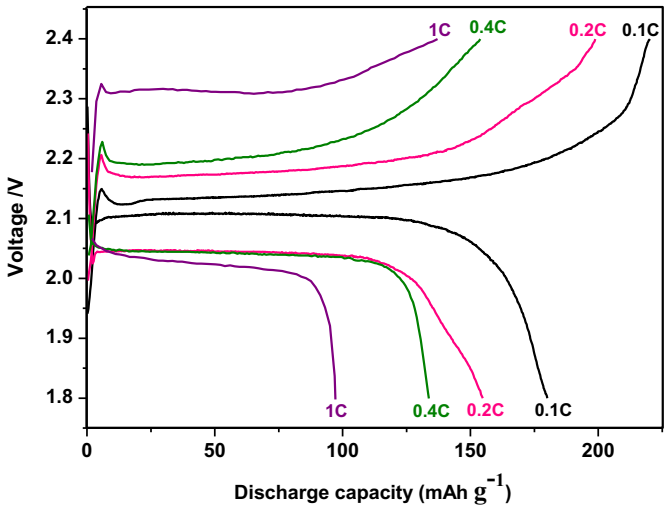

Fig. 6. Rate performance of urchin-like β-PbO_2 and flower-like α-PbO_2 in the ratio of 1:1.

After 100 cycles, the rate performance of the electrode made with urchin-like β-PbO_2 and flower-like α-PbO_2 in the ratio of 1:1 was evaluated at progressively increasing current densities following symmetric rates of charge and discharge. The rates were increased starting with 0.1 C to 0.2 C, 0.4 C, and as high as 1 C. And the resulting charge/discharge curves are presented in Fig. 6. The discharge capacity of 154.8 mA h g^{-1} and 133.7 mA h g^{-1} can be obtained at 0.2 C and 0.4 C, respectively. Unexpectedly, even at 1 C the electrode was still able to deliver a capacity of 97.2 mA h g^{-1}. The rate behavior of our sample is better than the other reports [28,29], and the progress achieved here can be ascribed to the thin film electrode adopted in our experiment. In this type of electrode, the contact area between the active material and the current collector is increased, just like the former report [30].

4. Conclusions

Nanostructured urchin-like and ball-like β-PbO_2, flower-like α-PbO_2 were chemically synthesized. The crystal phase, morphology and microstructure of the as-prepared samples can greatly affect the electrochemical properties of the electrode. The flower-like α-PbO_2 with lager particle size in positive active materials will help to construct the frame structure and form a conductive network in the electrode. The urchin-like β-PbO_2 with particular hollow and radial nanorods structures can improve the contact area with the electrolyte, offer unique advantages for electrolyte storage and make fast diffusion of H^+ and SO_4^{2-} ions in the electrode. In addition, the constant voltage charge step can accelerate the conversion of partial α-PbO_2 to β-PbO_2 and built up the connection between particles. More importantly, the hydrated zones can be formed in the PbO_2 particles during cycling and subsequently involved in the electrochemical processes of charge and discharge. Due to the above four factors, the electrodes would be able to present the increased discharge capacities. Moreover, the pretreatment is also important for the electrode, which will help to establish connections within the active materials and improve the stability of cycle. Our experimental results indicate that it should be possible to construct a thin film electrode with high discharge capacity, good cycling stability and excellent rate performance using chemically synthesized PbO_2. Nevertheless, it still is a challenge to find the more proper pretreatment process and charge method to improve the initial cycle performance. And the thin film electrode technology possibly sheds light on a new type of nanostructure-based lead-acid battery, which deserves more extensive research in the future.

Acknowledgment

This work was financially supported by the 973 Project of China (No. 2011CB935901) and China Postdoctoral Science Foundation (No. 2013M531514).

References

[1] P. Simon, Y. Gogotsi, Nat. Mater. 7 (2008) 845–854.
[2] J. Leadbetter, L.G. Swan, J. Power Sources 216 (2012) 376–386.

[3] H.J. Bergveld, D. Danilov, P.H.L. Notten, V. Pop, P.P.L. Regtien, in: J. Garche (Ed.), Encyclopedia of Electrochemical Power Sources, vol. 1, Elsevier, 2009, p. 459.
[4] Z. Yang, J. Zhang, M.C.W. Kintner-Meyer, X. Lu, D. Choi, J.P. Lemmon, J. Liu, Chem. Rev. 111 (2011) 3577–3613.
[5] L.T. Lam, R. Louey, J. Power Sources 158 (2006) 1140–1148.
[6] P.T. Moseley, J. Power Sources 191 (2009) 134–138.
[7] D. Pavlov, P. Nikolov, T. Rogachev, J. Power Sources 196 (2011) 5155–5167.
[8] D.A.J. Rand, J. Power Sources 28 (1989) 107–111.
[9] V.H. Dodson, J. Electrochem. Soc. 108 (1961) 401–405.
[10] A.C. Simon, E.L. Jones, J. Electrochem. Soc. 109 (1962) 760–770.
[11] D. Pavlov, G. Papazov, J. Electrochem. Soc. 127 (1980) 2104–2112.
[12] V.H. Dodson, J. Electrochem. Soc. 108 (1961) 406–412.
[13] D. Pavlov, Lead-acid Batteries: Science and Technology, Elsevier, 2011, p. 459.
[14] W.U. Huynh, J.J. Dittmer, A.P. Alivisatos, Science 295 (2002) 2425–2427.
[15] J. Morales, G. Petkova, M. Cruz, A. Caballero, J. Power Sources 158 (2006) 831–836.
[16] M. Bervas, M. Perrin, S. Geniès, F. Mattera, J. Power Sources 173 (2007) 570–577.
[17] P. Rüetschi, J. Electrochem. Soc. 139 (1992) 1347–1351.
[18] J. Morales, G. Petkova, M. Cruz, A. Caballero, Electrochem. Solid State Lett. 7 (2004) A75.
[19] P.T. Moseley, N.J. Bridger, J. Electrochem. Soc. 131 (1984) 608–610.
[20] R. Fitas, L. Zerroual, N. Cheladi, B. Djellouli, J. Power Sources 58 (1996) 225–229.
[21] J. de Andrade, P.R. Impinnisi, D.L. do Vale, J. Power Sources 196 (2011) 4832–4836.
[22] C.Y. Cui, X.M. Ma, D.L. Kong, H.Y. Ma, J. Electrochem. 19 (2013) 43–51.
[23] D. Pavlov, I. Balkanov, J. Electrochem. Soc. 139 (1992) 1830–1835.
[24] D. Pavlov, J. Electrochem. Soc. 139 (1992) 3075–3080.
[25] D. Pavlov, Lead-acid Batteries: Science and Technology, Elsevier, 2011, pp. 469–475.
[26] I. Petersson, E. Ahlberg, J. Power Sources 91 (2000) 137–142.
[27] T. Chen, H. Ma, D. Kong, Mater. Lett. 90 (2013) 103–106.
[28] P. Gao, Y. Liu, X. Bu, M. Hu, Y. Dai, X. Gao, L. Lei, J. Power Sources 242 (2013) 299–304.
[29] P. Gao, W. Lv, R. Zhang, Y. Liu, G. Li, X. Bu, L. Lei, J. Power Sources 248 (2014) 363–369.
[30] A. Caballero, M. Cruz, L. Hernán, J. Morales, L. Sánchez, J. Power Sources 113 (2003) 376–381.